

Optimization of PWM for Overmodulation Region of Two-level Inverters

Péter Stumpf

Dept. of Automation and Applied Informatics (AAI)
Budapest University of Technology and Economics,
MTA-BME Control Engineering Research Group
stumpf@aut.bme.hu

Sándor Halász

Dept. of Electric Power Engineering
Budapest University of Technology and Economics
halasz.sandor@vet.bme.hu

Abstract—Two optimized PWM techniques for the overmodulation region of two-level inverter-fed ac drives are investigated from harmonic loss minimization point of view. The optimization is elaborated for the lowest loss-factor, which is proportional to the square of rms value of current harmonics. The loss-factors are computed for different switching numbers as the function of the motor fundamental voltage. It is shown that, respect to the motor heating and torque ripples, the acceptable drive condition can be guaranteed by relatively low value of inverter switching frequency up to 96-97% of maximal possible motor voltage. Furthermore, it is shown that, the so-called Three vector method, introduced in the paper, has considerably better performance in the lower part of the overmodulation region than the so-called Two vector method or the standard PWM techniques for the same number of switching. The theoretical results are verified by experimental tests.

I. INTRODUCTION

Pulse Width Modulated (PWM) three phase two-level voltage source inverter (VSI) is one of the most common power converter topology in ac motor drive applications. In the last decades investigation of PWM techniques have been a hotspot in controlling of VSI as they are directly related to the efficiency of the overall system affecting the economical profit and performance of the final product.

The peak of the maximum output phase voltage of a three phase two-level VSI in the so-called six-step or square-wave mode of operation is limited to $U_{1max} = 4U_{DC}/\pi$, where $2U_{DC}$ is the DC-link voltage of the inverter. By operating the widely applied standard PWM techniques, like Space Vector Modulation (SVM) or Discontinuous PWM (DPWM) methods, in the so-called linear region, only the 90.7% of U_{1max} can be reached. Therefore, to improve the DC-link utilization and expanding the output voltage to U_{1max} the VSI should be operated in the overmodulation region.

Assuming that, the VSI is supplied through a diode bridge rectifier operating in continuous conduction mode the DC-link voltage in ideal case can be expressed as $2U_{DC} = 3/\pi \hat{U}_{LL}$, where \hat{U}_{LL} is the amplitude of the input line-to-line voltage. Hence, the maximum voltage output phase voltage at the border of linear modulation is $U = 0.907 \cdot 6\sqrt{3}/\pi^2 (\hat{U}_{LL}/\sqrt{3}) = 0.955(\hat{U}_{LL}/\sqrt{3})$. So ac motors of series production rated at the input line voltage would not reach rated operating point in the linear region. It means that, by taking into consideration the voltage drop in rectifier as well, more than 5% of the power is inaccessible from a motor fed from a VSI operated only in linear region [1], [2]. Consecutively, the

rated operational point and the flux weakening area of a mass-produced induction motor rated at the voltage of the AC input are in the overmodulation region. Thus the quality of the drive in this region is of great importance.

Operating VSI in overmodulation region is still an intensively studied field among researchers. Paper [3] introduces a predictive overmodulation technique in medium-voltage inverters operating at low switching frequencies. A general SVM procedure for overmodulation is described for n -phase drives, where n is an odd number, in [4]. Similarly to [4] SVM technique in overmodulation range is studied in [5], where a novel single-zone algorithm is introduced for two-level inverters, which significantly reduces the computational effort comparing to the standard two-zone algorithm. Overmodulation region of inverters are thoroughly studied in closed loop application [6], [7], [8]. Paper [6] introduces an overmodulation method in direct torque controlled induction machine drives to obtain a fast dynamic torque response, when the switching frequency is constant. A novel harmonic estimator, which eliminates the unavoidable low order harmonics causing problems in vector controlled drives is described in [7]. Paper [8] presents an overmodulation scheme for sinusoidal PWM used in Field Oriented Controlled (FOC) traction drives, when the switching frequency is only a few hundred Hertz. Overmodulation region of PWM techniques has key importance not only in motor drives but also in grid connected inverters. An overmodulation strategy has been proposed, tested and verified for a 250 kW grid-connected Photovoltaic inverter in [9].

The loss-optimized PWM methods for ac drives have been investigated since the seventies of last century [10], [11], [12], [13], [14]. Nowadays, thanks to the high performance digital devices the implementation of these methods is considerably simpler allowing their wider spread in practice. Probably in the first time it will be used only in overmodulation region where the today used standard PWM methods require some corrections (e.g. on pulses dropping etc.).

II. STATE OF THE ART

A. Loss-factor

The motor harmonic losses of the overmodulation region are generally characterized by the loss-factor [15], which for the pure inductive load is as follows

$$K'_{\Psi} = (L')^2 \sum_{\nu>1}^{\infty} I_{\nu}^2 = \Psi^2 - 1 = \sum_{\nu>1}^{\infty} \frac{U_{\nu}^2}{\nu^2}, \quad (1)$$

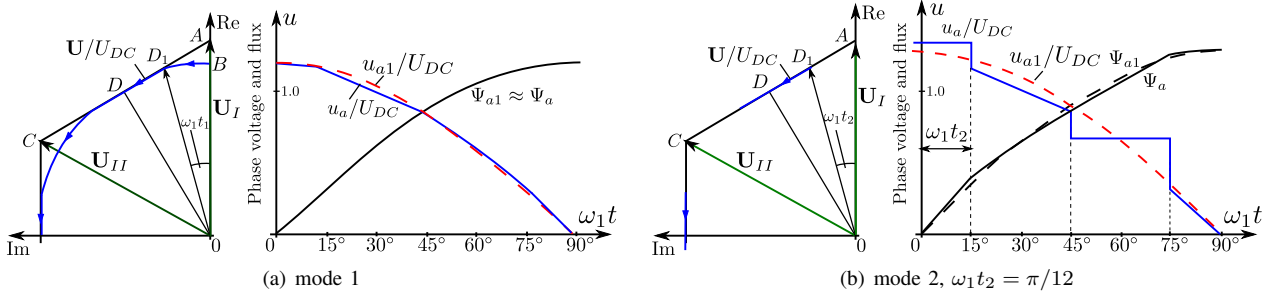


Fig. 1. Voltage vector path and phase voltage and flux versus time

where I_ν and U_ν are the current and voltage harmonics of the order ν , respectively. L' is the stator transient inductance, Ψ is the rms value of the stator flux and all the values are in pu system. The base values of pu system are the rated phase current and voltage, for the flux the ratio $U_{rated}/\omega_{1rated}$ (where ω_{1rated} is the electric synchronous angular velocity) and for the impedance U_{rated}/I_{rated} . Later on, we will use the relative loss-factor $K_\Psi = K'_\Psi/0.00215$, where $K'_\Psi = 0.00215$ is the loss-factor of the inverter operating in six-step mode [15].

B. Optimum solution

The optimum solution means the determination of loss-factor in case of infinitely high switching frequency of the VSI. In overmodulation region, for the fundamental voltage $U_1/U_{max} > 0.907$ the optimized increase of the voltage can be performed according to [15], [16], [17]. According to the magnitude of U_1/U_{1max} , two operational modes are possible. In the first mode the motor voltage vector \mathbf{U} moves along the circle BD_1 (Fig.1(a)) with fundamental angular velocity ω_1 until it reaches in the t_1 time the point D_1 of AC line. Then the voltage vector moves along the line D_1D with the same angular velocity ω_1 and at the moment $\pi/(6\omega_1)$ the vector will be in D point. The maximal fundamental voltage of the first operational mode is $0.9512U_{max}$ and takes place when D_1 point coincides with A point.

In the second operational mode of the investigated $\pi/6$ duration the $\mathbf{U} = \pi U_{1max}/3$ constant voltage vector stays in the point A for the time t_2 (Fig.1(b)). At t_2 the voltage vector turns by angle $\omega_1 t_2$ in D_1 point and moves along D_1D line with the constant angular velocity ω_1 . From Fig.1(b) it can be seen that the difference between the phase voltage or flux and their fundamental components become sensible. Therefore, the voltage harmonics and current harmonic losses of this operational mode reach significant values. The angles $\omega_1 t_1$ and $\omega_1 t_2$ as the function of the fundamental voltage U_1/U_{1max} can be seen on Fig.2(a).

The loss-factor is drawn in Fig.2(b). This loss-factor curve is computed as $\Psi^2 - 1$ by numerical integration of Ψ flux vector [15]. In the first operational mode the loss-factor is very low. Therefore, it is impossible to distinguish the phase flux from its fundamental component as it can be seen on Fig.1(a) (the flux is given in voltage scale). The maximal $K_\Psi = 0.024$ value of this mode belongs to $U_1/U_{1max} = 0.9514$.

The first eight harmonic voltage components (with correct sign of vector presentation) are presented in Fig.3. Only harmonics of order $\nu = 1 \pm 6K$ are possible ($K = 0, 1, 2, 3, \dots$). From Fig.3 it can be seen that, in the first operational mode the

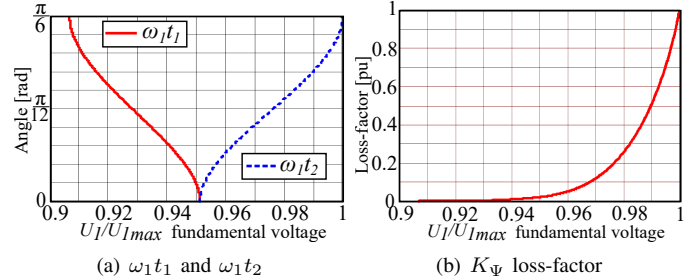


Fig. 2. $\omega_1 t_1$ and $\omega_1 t_2$ angles and K_Ψ loss-factor as the function of U_1/U_{1max}

voltage harmonics for the same K have the same amplitude. The motor harmonic losses as well as the torque pulsation are mainly determined by harmonic currents of order -5 and 7 . These losses decrease sharply with decrease of the motor voltage. However, the motor torque pulsation really decreases only in the first operational mode. This is clear from Fig.3 since the torque of order 6 is determined by sum of the torques from currents of order -5 and 7 . These torque components have different sign for different sign of voltage harmonics in the second operational mode.

It should be noted that, the conclusions presented previously, assuming infinitely high switching frequency, are valid for multi-level inverters too. Thus, it is impossible to obtain better results than presented above (Fig.2(b)). Naturally, this statement is not true, when the switching frequency is a finite number.

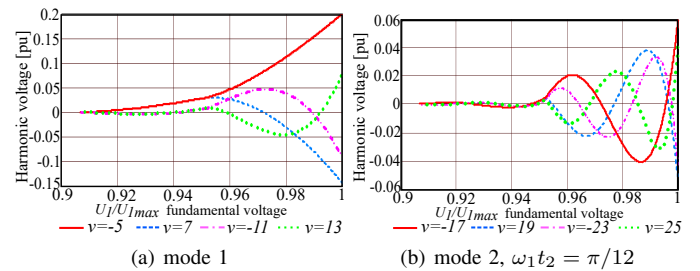


Fig. 3. Harmonic voltages for infinitely high switching frequency ($\gamma = \infty$)

III. OPTIMIZATION OF PWM FOR OVERMODULATION REGION

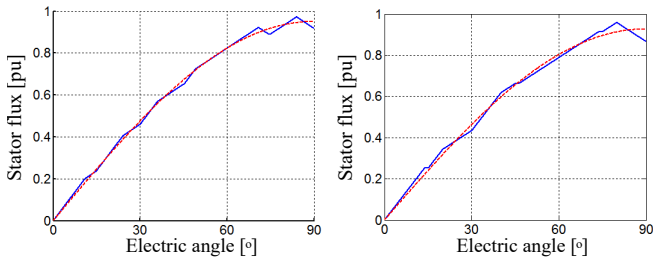
The computation problem was investigated also in [1], [10], [11], [12]. For a given number of inverter switching and a desired V fundamental voltage the Lagrange function

$$F = \frac{\Psi^2}{\Psi_1^2} - 1 + \lambda(U_1^2 - V^2) \quad (2)$$

must be minimized, where F depends on τ_i switching (commutation) angles and on λ . The computation uses Newton-Raphson method. The computation starts from a given value of V and a selected voltage vector row as well as initial switching angles. It continues until all the first derivatives of F become close to zero. Due to the symmetry of vector paths computations were performed only for $0 \leq \omega_1 t \leq \pi/6$ sector (Fig.1), where only $\mathbf{U}_I = \frac{4}{3}U_{DC}$ and $\mathbf{U}_{II} = \mathbf{U}_I e^{j\pi/3}$ and zero voltage vectors used.

The computations were performed for different number of switching on $1/6^{th}$ of the fundamental period: $\gamma = 5, 7, 9, 11, 13, 21, 31$. For a given γ the number of applying voltage vectors is $(\gamma + 1)/2$, the number of varying switching angles is $(\gamma - 1)/2$, the total number of parameters with $\tau_1 = 0$, $\tau_{(\gamma+1)/2} = \pi/6$ and λ is $(\gamma - 1)/2 + 3$.

For demonstration the situation for $\gamma = 7$ is presented in Fig.4 where the voltage vector row in Fig.4(a) is $\mathbf{U} = [\mathbf{U}_I, \mathbf{U}_{II}, \mathbf{U}_I, \mathbf{U}_{II}]$ while in Fig.4(b) it is $\mathbf{U} = [\mathbf{U}_I, 0, \mathbf{U}_I, \mathbf{U}_{II}]$. The stator phase flux and its fundamental component are presented for $U_1 = 0.95U_{1max}$ (Fig.4(a)) and for $U_1 = 0.92U_{1max}$ (Fig.4(b)). Later on the first case, when zero voltage vector is not applied, is called *Two vector method*, and the case, when zero voltage vector is also applied is called *Three vector method*.



(a) $U_1 = 0.95U_{1max}$, two vector method (without zero vector) (b) $U_1 = 0.92U_{1max}$, three vector method (with zero vector)

Fig. 4. Stator phase flux (blue line) and its fundamental component (dashed line), $\gamma = 7$

A. Two vector method - "High voltage region"

This region corresponds to the operation mode 2 in 1(b). The voltage vector path never moves along a fundamental voltage vector path. Therefore, only the two active voltage vectors can be used to obtain a loss-optimal PWM control. Thus, the zero voltage vectors are not used in this case. The method is introduced in [11].

The loss-factors for $\gamma = 5, 7, 9, 11, 13$ and $\gamma = 21, 31$ are given in Fig.5(a) and in Fig.5(b), respectively. In practice it is desirable to obtain a K_Ψ loss-factor value lower than 0.1 as usually in this case an underrating of the motor is not necessary. According to Fig.5 the loss-factor is lower than 0.1 only in narrow region of the motor voltage. The performance can be improved by increasing γ , however even for $\gamma = 31$ it is not possible to obtain loss-factor under 0.1 for the whole overmodulation range.

In Fig.6(a) the voltage harmonics of order $\nu = -5, 7, -11$ and 13 are drawn for $\gamma = 13$. For this case, when $U_1 \leq 0.934U_{1max}$ the first switching angle $\tau_2 = 0$, but γ stays 13

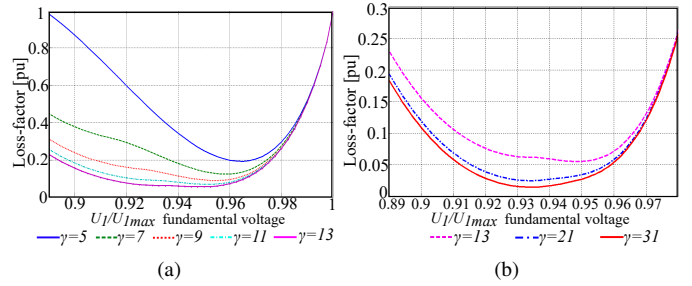
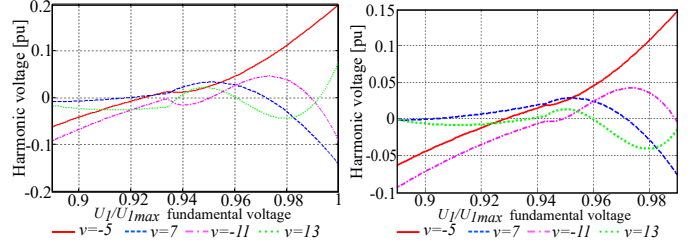


Fig. 5. K_Ψ loss-factor as the function of U_1/U_{1max} , Two vector method



(a) $U_1 = 0.95U_{1max}$, two vector method (without zero vector) (b) $U_1 = 0.92U_{1max}$, three vector method (with zero vector)

Fig. 6. Harmonic voltages, Two vector method

since at $t = 0$ there are two switchings (one-one in phases b and c). Figure 6(b) presents the voltage harmonics for $\gamma = 31$.

Based on Fig.6 and Fig.3 it can be concluded that, in the $U_1 \geq 0.95U_{1max}$ region the voltage harmonics have practically the same values for $\gamma = 13$ (Fig.6(a)), $\gamma = 31$ (Fig.6(b)) and for infinitely high switching frequency ($\gamma = \infty$, Fig.3). Thus, it is worth to optimize the PWM only in the low voltage region. Furthermore, as the increase of the switching frequency does not change the amplitude of the low order harmonics in the $U_1 \geq 0.95U_{1max}$ region, it is impossible to decrease the torque pulsation in sensible rate in this region.

B. Three vector method - "Low voltage region"

This region corresponds to the operation mode 1 in 1(a). The voltage vector path from $t = 0$ is moving along \mathbf{U}_1 vector path, therefore the zero voltage vectors should be used as well. As it will be shown later by using the zero voltage vectors the loss-factor values, at least in important part of voltage region, can be decreased.

The zero voltage vectors should be applied in initial part of the voltage vector row. Therefore there are two possible voltage vector row: $\mathbf{U} = [0, \mathbf{U}_I, \mathbf{U}_{II}, \mathbf{U}_I, \mathbf{U}_{II}, \dots]$ and $\mathbf{U} = [\mathbf{U}_I, 0, \mathbf{U}_I, \mathbf{U}_{II}, \mathbf{U}_I, \mathbf{U}_{II}, \dots]$. In the current paper the latter one will be studied in more detail.

The results of computations for $\gamma = 13$ and 31 are presented in Fig.7 and 8, respectively. The selected voltage vector row is $\mathbf{U} = [\mathbf{U}_I, 0, \mathbf{U}_I, \mathbf{U}_{II}, \mathbf{U}_I, \mathbf{U}_{II}, \dots]$. For the better comparison the loss-factors applying two vector method are plotted on Fig.7 as well. It can be seen that, in low voltage region the loss-factor decreased comparing to the two vector method and the magnitude of low voltage harmonics became very close to the case of $\gamma = \infty$ (Fig.3). The broken points in Fig.8 denote the points where the duration of the zero voltage vector became zero consequently the switching number decreases by 4 (to 9 from 13 in Fig.8(a) and to 27 from 31 in Fig.8(b)).

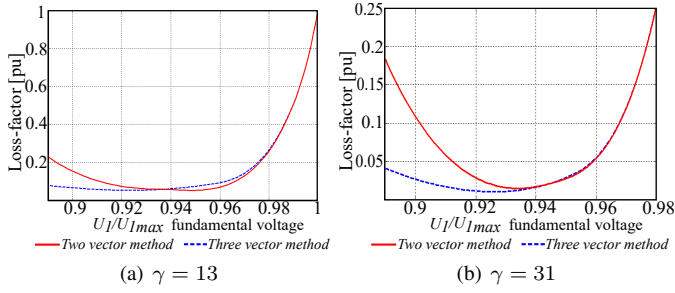


Fig. 7. Comparison of K_{Ψ} loss-factor as the function of U_1/U_{1max}

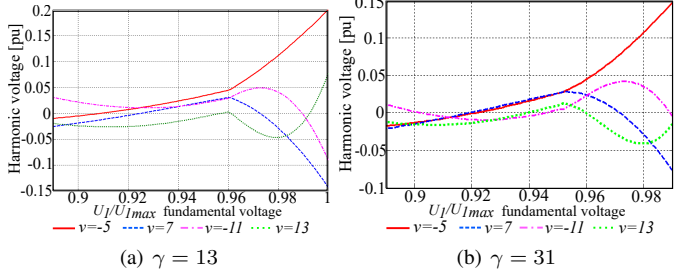


Fig. 8. Harmonic voltages, Three vector method

Probably for higher value of γ more zero voltage vectors should be used, but according to our calculations for $\gamma \leq 33$ even the use of two zero voltage vectors could not decrease the loss-factor further.

IV. TORQUE PULSATIONS

The motor torque pulsation is computed by neglecting the motor stator and rotor resistances. In this case the harmonic currents are restricted only by the stator transient reactance therefore the motor torque pulsation is determined with a good approximation according as follows:

$$\Delta m = (\Psi_1 - \mathbf{I}_1 L') \times \Delta \mathbf{i}, \quad (3)$$

where Ψ_1 and \mathbf{I}_1 is the stator fundamental flux and stator current, respectively. L' is the transient reactance and $\Delta \mathbf{i}$ is the harmonic current vector. In synchronous rotated coordinate system under no-load condition the first term in (3) aligns along imaginary axis. Therefore

$$\Delta m = (\Psi_1 - I_1 L') \cdot \Delta \text{Re}[\mathbf{i}] \quad (4)$$

By assuming $\Psi_1 = 1$, $I_1 = 0.5$ and $L' = 0.14$, the first term is 0.93.

The torque time function is drawn in Fig.9 for $\gamma = 13, 31$ and $\gamma = \infty$. It can be seen that, the increase off switching number can not decrease the 6th torque component effectively. At the same time, as it was expected based on the previous chapter, the use of three vector method leads to an effective decrease of higher order torque components comparing to the two vector method in the lower voltage region ($U_1 < 0.95U_{1max}$). The frequencies of these two dominant components are $3(\gamma \pm 1)f_1$, where f_1 is the fundamental frequency.

V. EXPERIMENTAL RESULTS

To verify the calculation results just described, laboratory measurements were carried out. Both the two vector and the three vector method were implemented in a low-cost 16-bit Digital Signal Controller (dsPIC33EP512MU810). A commercially available three-phase IGBT module from company Fairchild (FSBB30CH60C) was used for the tests. The DC link voltage and the dead time were $2U_{DC} = 90$ V and $2\mu s$, respectively.

The measurements were carried on an induction machine with rated speed 18 krpm. The rated data and main parameters of the machine are: power: $P_N = 3$ kW, rms line-to-line voltage $U_{LL,RMS} = 380$ V, phase rms current $I_{N,RMS} = 7.7$ A, rated frequency $f_{1N} = 300$ Hz, stator and rotor resistance $R_S = 1.125\Omega$, $R_R = 0.85\Omega$, stator and rotor leakage reactance $X_{LS} = 4.71\Omega$ and $X_{LR} = 2.63\Omega$, magnetizing reactance $X_m = 84.82\Omega$ (all reactance are at rated frequency) and the number of pole pairs is $p = 1$.

The experimental results at no-load are shown in Fig.10. For simplicity, the measurements were carried out at lower fundamental frequencies than the rated one. The motor was started using Space Vector Modulation (SVM) algorithm by keeping the stator flux constant ($U_1/f_1 = \text{const}$). The overmodulation region was reached at $f_1 = 45$ Hz, where $U_1 = 0.9U_{1max}$. Over $f_1 = 45$ Hz the two proposed optimal PWM strategies were applied.

Figure 10(a) and 10(b) present the time function of the motor phase voltage, motor phase current, the torque pulsation and the harmonic spectra of the phase voltage at $f_1 = 45$ Hz and $\gamma = 13$ ($U_1 = 0.9U_{1max}$) for the two vector and the three vector method, respectively. For the better comparison the same results were depicted for SVM as well on Fig.10(c). The switching frequency for SVM was $13 \cdot 45 = 585$ Hz to obtain the same number of switching over one fundamental period. As it can be seen, the three vector method has superior performance over the two vector method and SVM algorithm. The amplitudes of the higher harmonics are considerably lower. Furthermore, the peak-to-peak value of the torque pulsation is practically half by comparing it with the two vector method. The results are in line with the calculated one presented in the previous section (see Fig.9). By increasing the fundamental frequency and U_1 the difference between the two vector and three vector method becomes negligible. Figure 10(d) and 10(e) show experimental results for $U_1 = 0.96U_{1max}$ ($f_1 = 48$ Hz). It can be seen that, the harmonic performance of the two vector method is better than the three vector method. However, it should be noted, over $U_1 = 0.96U_{1max}$ (for $\gamma = 13$) the duration of the zero voltage vector became zero consequently γ decreases by 4, so $\gamma = 9$ on Fig.10(e). It results in lower switching loss comparing it with the two vector method presented on Fig.10(d).

VI. CONCLUSIONS

Two harmonic loss-optimized PWM control methods in overmodulation region of three phase inverter-fed ac drives are investigated. It is shown that, the two vector method, which not utilize the zero voltage vectors is able to produce an optimized control only in the upper part of overmodulation region. By

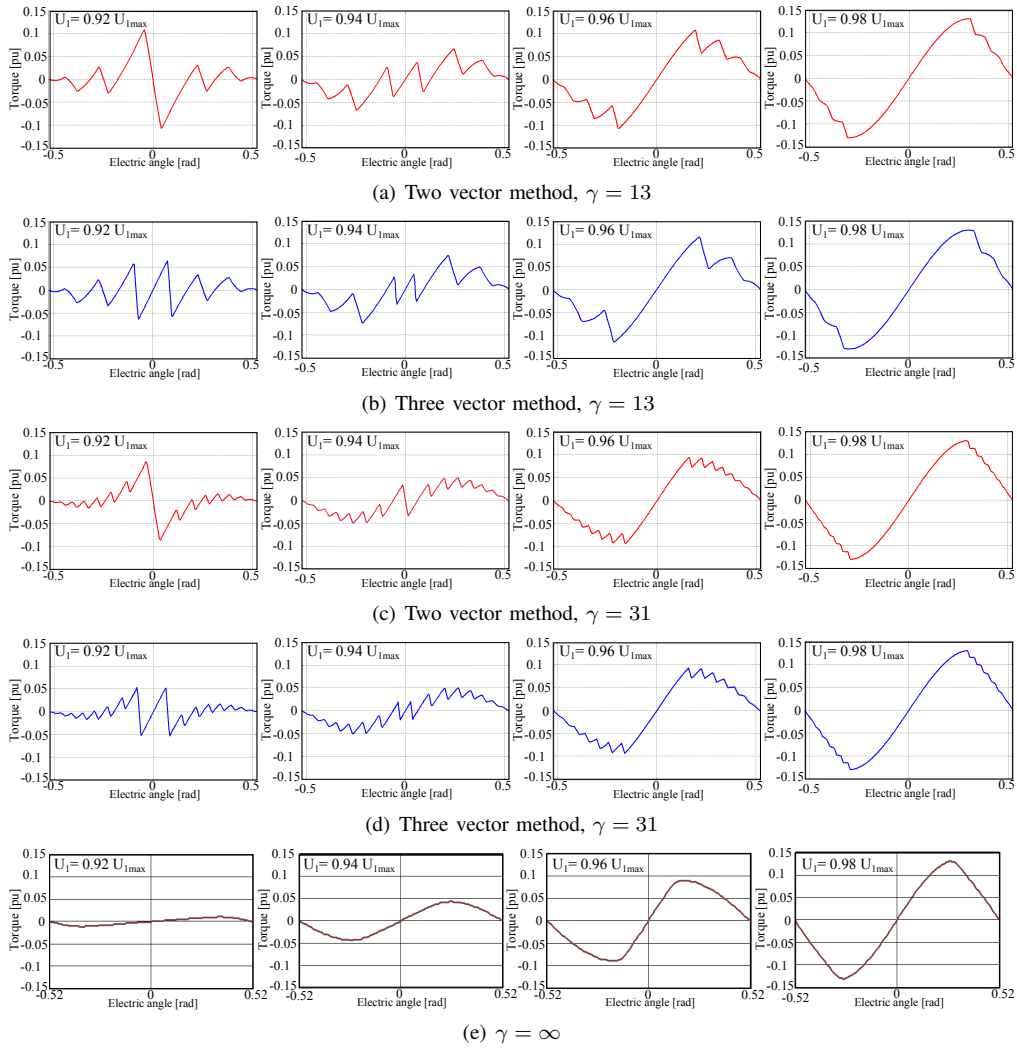


Fig. 9. Torque pulsation at no-load

using zero voltage vector (Three vector method) in the lower part ($U_1 \leq 0.9514U_{1max}$) of the overmodulation region a considerably better performance can be obtained.

The optimized control for both method is computed for number of inverter switching $\gamma = 5, 7, 9, 11, 13, 21, 31$ on 1/6th of fundamental period. Investigation of the drive with these switching numbers has shown:

a) Motor harmonic losses in the range of $0.98U_{1max} \leq U_1 \leq U_{1max}$ virtually independent on the number of inverter switching. When $0.9U_{1max} \leq U_1 \leq 0.96U_{1max}$ and the number of switching $\gamma \geq 13$ the motor harmonic losses will be so small that the influence of these losses on motor heating can be neglected. The last is valid for $0.9U_{1max} \leq U_1 \leq 0.975U_{1max}$ if γ is increased to 31.

b) Motor torque pulsation and especially the torque of 6th order in case of $0.95U_{1max} \leq U_1 \leq U_{1max}$ can not be sensible decreased by increasing the switching number γ . Furthermore for $0.9U_{1max} \leq U_1 \leq 0.93U_{1max}$ the torque of 6th order becomes almost zero and only torque pulsation of high frequency becomes dominant.

The results of computations were checked by experimental tests.

ACKNOWLEDGEMENT

This paper was supported by the János Bolyai Research Scholarship of the Hungarian Academy of Sciences.

REFERENCES

- [1] D. G. Holmes and T. A. Lipo, *Pulse width modulation for power converters: principles and practice*. John Wiley & Sons, 2003, vol. 18.
- [2] A. M. Hava, R. J. Kerkman, and T. A. Lipo, "Carrier-based pwm-vsi overmodulation strategies: analysis, comparison, and design," *IEEE Trans. on Power Electronics*, vol. 13, no. 4, pp. 674–689, Jul 1998.
- [3] J. Holtz, "Advanced pwm and predictive control - an overview," *IEEE Trans. on Industrial Electronics*, vol. 63, no. 6, pp. 3837–3844, June 2016.
- [4] J. Prieto, F. Barrero, M. J. Durn, S. T. Marn, and M. A. Perales, "Svm procedure for n-phase vsi with low harmonic distortion in the overmodulation region," *IEEE Trans. on Industrial Electronics*, vol. 61, no. 1, pp. 92–97, Jan 2014.
- [5] M. K. Modi and G. Narayanan, "Improved single-zone overmodulation algorithm for space vector modulated inverters," in *Power Electronics, Drives and Energy Systems (PEDES), 2014 IEEE International Conference on*, Dec 2014, pp. 1–6.
- [6] A. Jidin, N. R. N. Idris, A. H. M. Yatim, T. Sutikno, and M. E. Elbuluk, "Simple dynamic overmodulation strategy for fast torque control in dtc of induction machines with constant-switching-frequency controller," *IEEE Trans. on Industry Applications*, vol. 47, no. 5, pp. 2283–2291, Sept 2011.

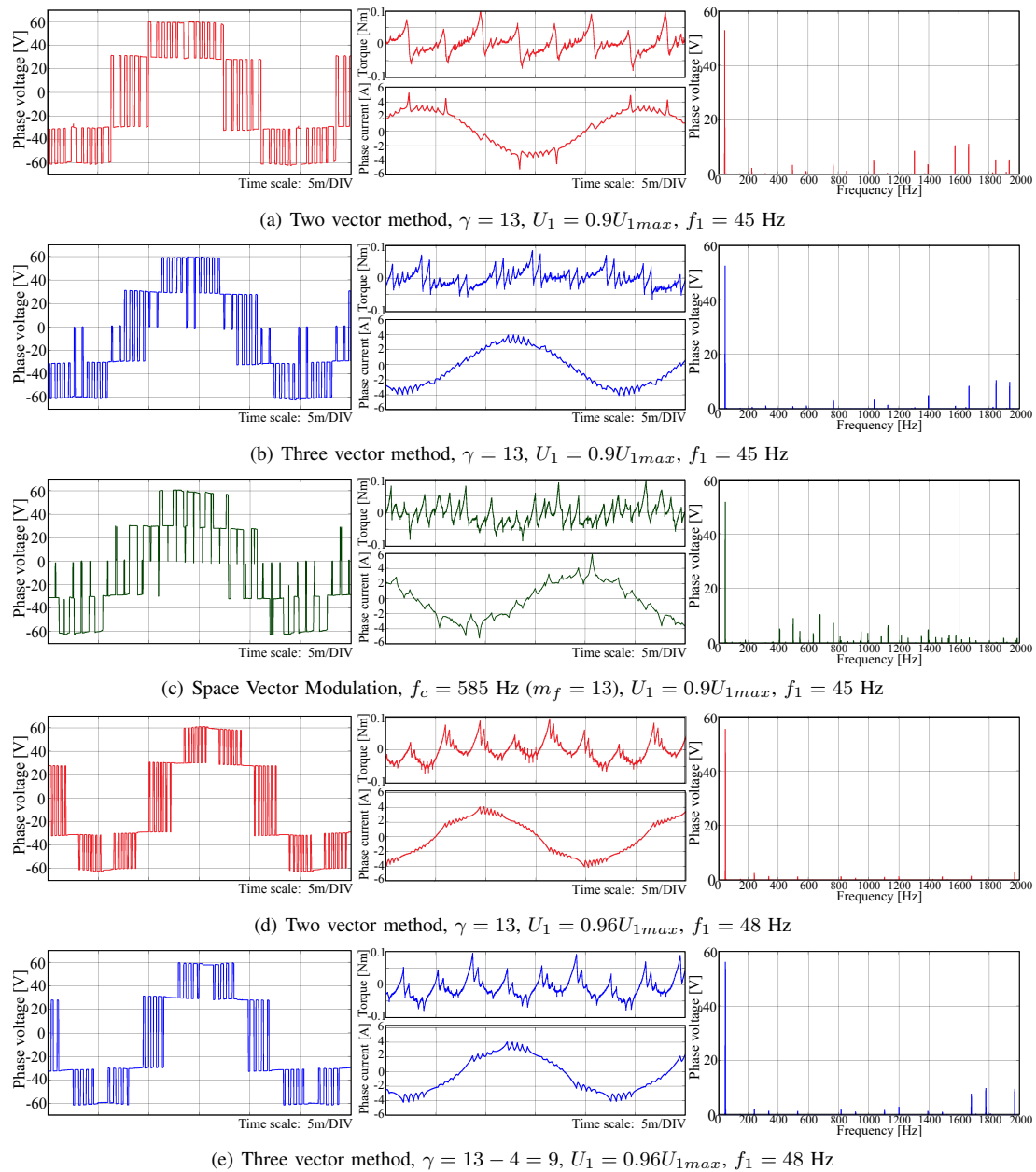


Fig. 10. Experimental test results at no-load, time function of phase voltage (left), time function of phase current and torque signal (middle) and harmonic spectra of phase voltage (right)

- [7] K. Kondo and S. Doki, "Improvement of transient state characteristic for vector control system by using the inverter overmodulation range," in *Power Electronics and Applications (EPE'15 ECCE-Europe), 2015 17th European Conference on*, Sept 2015, pp. 1–7.
- [8] T. B. S. K. Sahoo, "Rotor flux-oriented control of induction motor with synchronized sinusoidal pwm for traction application," *IEEE Trans. on Power Electronics*, vol. 31, no. 6, pp. 4429–4439, June 2016.
- [9] Y. Park, S. K. Sul, and K. N. Hong, "Linear over-modulation strategy for current control in photovoltaic inverter," in *2014 International Power Electronics Conference (IPEC-Hiroshima 2014 - ECCE ASIA)*, May 2014, pp. 2598–2605.
- [10] G. S. Buja and G. B. Indri, "Optimal pulsewidth modulation for feeding ac motors," *IEEE Trans. on Industry Applications*, vol. IA-13, no. 1, pp. 38–44, Jan 1977.
- [11] S. Halasz, "Optimized control of pwm inverters for a given number of commutations (in hungarian)," *Elektrotechnika*, vol. 76, no. 10-11, pp. 386–391, March 1983.
- [12] —, "Selection of reasonable commutation frequency of inverters for ac drives," in *Proceedings of International Conference on Electrical Machines*, 1986, pp. 991–994.
- [13] M. Bierhoff, H. Brandenburg, and F. W. Fuchs, "An analysis on switching loss optimized pwm strategies for three phase pwm voltage source converters," in *Industrial Electronics Society, 2007. IECON 2007. 33rd Annual Conference of the IEEE*, Nov 2007, pp. 1512–1517.
- [14] Q. Lei, D. Cao, and F. Z. Peng, "Novel loss and harmonic minimized vector modulation for a current-fed quasi-z-source inverter in hev motor drive application," *IEEE Trans. on Power Electronics*, vol. 29, no. 3, pp. 1344–1357, March 2014.
- [15] S. Halasz, I. Varjasi, and A. Zacharov, "Overmodulation strategies of inverter-fed ac drives," in *Power Conversion Conference, 2002. PCC-Osaka 2002. Proceedings of the*, vol. 3, 2002, pp. 1346–1351 vol.3.
- [16] D.-C. Lee and G.-M. Lee, "A novel overmodulation technique for space-vector pwm inverters," *IEEE Trans. on Power Electronics*, vol. 13, no. 6, pp. 1144–1151, Nov 1998.
- [17] J. Holtz, W. Lotzkat, and A. Khambadkone, "On continuous control of pwm inverters in the overmodulation range including the six-step mode," in *Proceedings of IECON 1992*, Nov 1992, pp. 307–312 vol.1.